An Efficient Broadband Decoupling Sequence for Liquid Crystals

Youlu Yu and B. M. Fung

Department of Chemistry and Biochemistry, University of Oklahoma, Norman, Oklahoma 73019-0370

A new and efficient broadband decoupling sequence is presented. It is based on the phase cycling of two pulses with small phase angles. The pulse width is 180° ± 30°, and the phase angle is ±10°–12°. The sequence contains 16 elements, and is called SPARC-16 as an abbreviation for *s*mall *p*hase *a*ngle *r*apid *c*ycling. The application of this sequence to a liquid crystalline compound, 4-*n*-pentyl-4′-cyanobiphenyl (5CB), is reported. The signal-to-noise ratios and the linewidths of the ^{13}C peaks of 5CB with SPARC-16 decoupling and with other decoupling methods are compared. The results show that the broadband decoupling efficiency of SPARC-16 is considerably better than those of other methods. © 1998 Academic Press

Key Words: broadband decoupling; liquid crystals; SPARC-16.

INTRODUCTION

Signal averaging and broadband decoupling are two essential techniques that have led to the wide application of NMR studies on ^{13}C and other ''rare'' nuclei. Since the first introduction of ''noise decoupling'' (*1*), many pulse sequences have been developed to improve the efficiency of heteronuclear decoupling in liquids. For example, decoupling sequences based on composite pulses with phase-modulation, such as MLEV (*2–5*), WALTZ (*6, 7*), and GARP (*8, 9*), have been proven to be very successful. Recently, adiabatic frequency-sweeping sequences have been developed (*10–18*) to offer another jump in the efficiency of heteronuclear decoupling in order to fulfill the demanding requirement of ultrahigh-field NMR spectrometers. Because these broadband decoupling sequences are specially designed for isotropic liquids, their applications in heteronuclear decoupling for solids and liquid crystals are far from satisfactory, primarily due to the existence of large dipolar interactions in these systems.

The most common method for heteronuclear decoupling in the solid state is to apply a high-power continuous-wave (CW) radiofrequency (RF) irradiation, the field strength of which is comparable to or greater than the magnitude of both homonuclear and heteronuclear dipolar interactions in the system (*19*). In an effort to reduce the power requirement for broadband decoupling in the solid state, Griffin and co-workers (*20*) have recently introduced a decoupling scheme called TPPM. This decoupling sequence contains two alternating pulses, $P = \tau_p(\phi/2)$ and $\bar{P} = \tau_p(-\phi/2)$, where τ_p is a short pulse of about 165°, and ϕ is a small phase angle. It was shown that the TPPM sequence can improve the efficiency of heteronuclear decoupling considerably over the conventional CW method.

The magnitude of dipolar coupling in liquid crystals is less than that in solids. On the other hand, the demand for efficient broadband decoupling is more stringent because high RF power causes an unacceptable effect which changes the order parameter of the liquid crystal being studied (*21*). About 10 years ago, several types of composite sequences were developed for broadband decoupling in liquid crystals (*22–25*), but there has not been much progress since then. Now we have found a phase-cycled version of the TPPM sequence that offers a much better efficiency than the known decoupling schemes for the broadband decoupling of liquid crystals, and the results are reported here. These decoupling pulse sequences are called SPARC because they undergo *s*mall *p*hase *a*ngle *r*apid *c*ycling during the acquisition time.

RESULTS AND DISCUSSION

The approach for constructing the SPARC sequences is to arrange the basic TPPM pulses P and $\bar{P}$ in phase cycling schemes according to well-documented methods (*4, 9*). The following are examples of some of the SPARC sequences:

$$\text{SPARC-4} = P\bar{P}\bar{P}P$$

$$\text{SPARC-8} = P\bar{P}\bar{P}P \ \bar{P}PP\bar{P}$$

$$\text{SPARC-16} = P\bar{P}\bar{P}P \ \bar{P}PP\bar{P} \ PP\bar{P}P \ \bar{P}\bar{P}P\bar{P}.$$

For example, SPARC-8 is a combination of two SPARC-4 sequences, with the second having opposite phases to the first. A SPARC-16 sequence can be constructed from two SPARC-8 sequences through a cyclic permutation, but avoiding the components PPP and $\bar{P}\bar{P}\bar{P}$ because they diminish the decoupling efficiency in practical testing. There are, of course, several possible ways to cycle the phases for SPARC-8 and SPARC-16. Depending on how they are constructed, these composite decoupling sequences show differ-
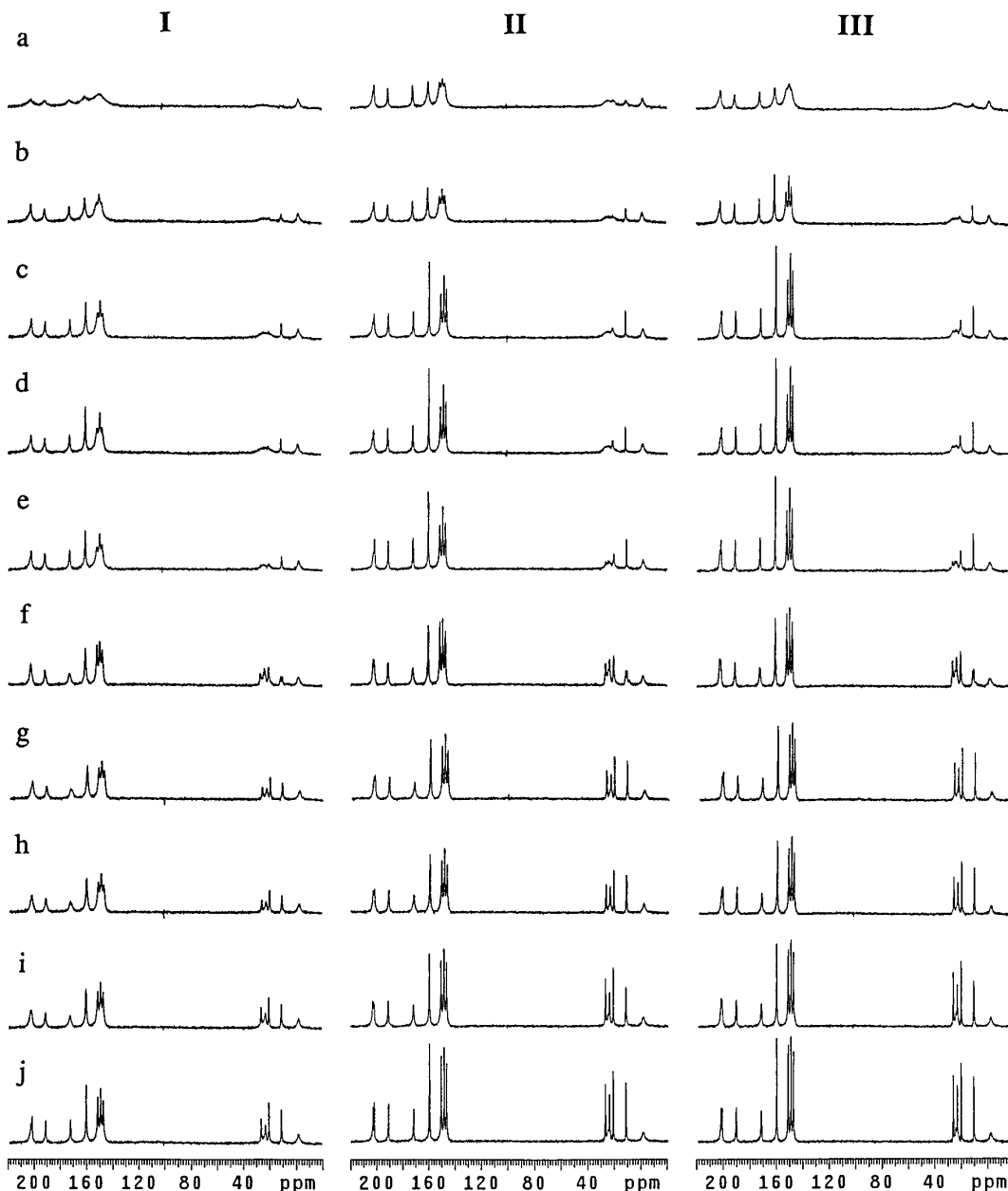
FIG. 1. ^{13}C NMR spectra of 4-n-pentyl-4$'$-cyanobiphenyl (5CB) at 9.4 T and ambient temperature. The decoupling power ($\gamma B_2/2\pi$) was the same for the spectra in each column: (I) 13 kHz; (II) 19 kHz; (III) 22 kHz. The decoupling sequences were: (a) GARP; (b) WALTZ-16; (c) ALPHA-3; (d) Waugh-3; (e) XY-32; (f) CW (continuous wave); (g) COMARO-2; (h) COMARO; (i) TPPM; and (j) SPARC-16. The peak assignment is (from left to right for decreasing chemical shifts in spectrum III-j) 4, 1$'$, 1, 4$'$, 3$'$, 3, 2$'$, 2, α, γ, β, δ, ω, and −CN.

ent efficiencies. The sequences given above are the most efficient versions. We have found that the SPARC-16 sequence shown above has the best decoupling efficiency. Further increase in the number of cycles did not improve the efficiency to any significant extent.

The decoupling efficiency of each SPARC sequence is dependent on the phase angle $\phi/2$. A systematic variation of ϕ showed that its optimal value lies between 20° and 25°.

A decrease in the decoupling efficiency of 20% or more was found for $\phi > 60°$. The exact width of the τ_p pulse is not critical, and it can be set to 180° ± 30° without significant change (<5%) in the decoupling efficiency.

To compare the efficiency of the broadband decoupling sequence SPARC-16 with those of the existing sequences, we chose to study the full ^{13}C NMR spectra of a bulk liquid crystal, 4-n-pentyl-4$'$-cyanobiphenyl (5CB), rather than ex-
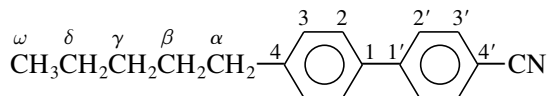
TABLE 1

Signal-to-Noise Ratios (S/N) for the Highest Peak in Each Region and Linewidths of the Best Resolved Peaks in the ^{13}C NMR Spectra of 5CB for Different Decoupling Sequences

Decoupling sequence	S/N		Linewidth (Hz)					Reference
	Aromatic	Aliphatic	1-Carbon	4′-Carbon	3′-Carbon	δ-Carbon	ω-Carbon	
GARP	23	7	88	86	146	na[a]	272	(8)
WALTZ-16	32	11	110	99	101	na[a]	64	(6)
ALPHA-3	65	28	75	71	45	200	39	(22)
Waugh-3	77	25	67	68	44	200	35	(26)
XY-32	51	30	64	70	49	84	36	(27)
CW	62	25	102	157	81	80	187	—
COMARO-2	47	45	89	156	67	40	42	(24)
COMARO	52	44	86	132	70	39	44	(24)
TPPM	71	52	80	101	54	36	47	(20)
SPARC-16	80	55	49	61	41	30	33	This work

Note. The decoupling power was $\gamma B_2/2\pi = 19$ kHz. The number of scans was 100, and no line broadening was used for data processing.

[a] Not available because the peak overlaps with other aliphatic peaks.

amining the peaks of a solute in a liquid crystal solvent, which is less technically demanding and has less practical significance. The structure of 5CB is

$$\underset{\omega}{CH_3}\underset{\delta}{CH_2}\underset{\gamma}{CH_2}\underset{\beta}{CH_2}\underset{\alpha}{CH_2}\text{—}\underset{4}{}\overset{3\ 2}{\bigcirc}\underset{1}{}\underset{1'}{}\overset{2'\ 3'}{\bigcirc}\underset{4'}{}\text{—CN}$$

The experiments were carried out with three levels of proton decoupling power: $\gamma B_2/2\pi = 13$, 19, and 22 kHz; the value of 13 kHz was the lowest possible to obtain reasonable broadband decoupling for this liquid crystal sample. The experiments were performed using a number of decoupling sequences, and the resulting ^{13}C spectra of 5CB are shown in Fig. 1. The overall quality of the spectra increases roughly in the order of GARP (8), WALTZ-16 (6), ALPHA-3 (22), Waugh-3 (26), XY-32 (27), CW, COMARO-2 (24), COM-

TABLE 2

Linewidths (Hz) of the Best Resolved Peaks in the ^{13}C NMR Spectra of 5CB for Three Decoupling Sequences with Varying Decoupling Power

$\gamma B_2/2\pi$ (kHz)	Decoupling sequence	1	4′	3′	δ	ω
13	COMARO	125	261	135	63	88
	TPPM	129	200	105	56	56
	SPARC-16	62	74	62	38	44
19	COMARO	86	132	70	39	44
	TPPM	80	101	54	36	47
	SPARC-16	49	61	41	30	33
22	COMARO	73	121	57	34	37
	TPPM	80	102	51	34	44
	SPARC-16	83	74	43	29	32

ARO (24), TPPM (20), and SPARC-16. Although the sequences GARP and WALTZ-16 are very efficient for isotropic liquids, they do not decouple 5CB well (Figs. 1a and 1b). It is interesting that the GARP sequence, which is better than WALTZ-16 for liquids, actually performs worse for liquid crystals. Its efficiency increases when the decoupler power is increased from 13 to 19 kHz, but does not improve further when the power is increased to 22 kHz; the reason for this is not clear to us, but we noticed that it is much more sensitive to the setting of the $\pi/2$ pulse width than other sequences tested. The decoupling sequences ALPHA-3, Waugh-3, and XY-32 (Figs. 1c, 1d, and 1e, respectively) yield relatively narrow aromatic and CH$_3$ peaks, but do not give good decoupling for the other aliphatic carbons. CW decoupling (Fig. 1f) gives reasonable decoupling for all peaks except the methyl carbon. COMARO-2 and COMARO, which were specially designed for heteronuclear decoupling of oriented materials, yield sharper peaks for every carbon (Figs. 1g and 1h), but are not as good as TPPM (Fig. 1i). The new sequence SPARC-16 shows the best result (Fig. 1j), and all the peaks have smaller linewidths and significantly larger intensities than those in the other spectra in Fig. 1.

To document the decoupling efficiencies of different broadband decoupling methods quantitatively, the signal-to-noise ratios (S/N) in both the aromatic and aliphatic regions and the linewidths of five of the well-resolved peaks for 5CB are tabulated in Table 1 for $\gamma B_2/2\pi = 19$ kHz. As in Fig. 1, the order in the table is arranged roughly according to the overall quality of the spectra; it does not always correspond to S/N or the inverse of the linewidths of the best-resolved peaks. Furthermore, it is to be noted that the signal-to-noise ratio in each region was measured with respect to the highest peak in that region, and is not necessarily related to any of the tabulated linewidth values. Nevertheless, the data in Table 1

clearly show that SPARC-16 is superior to all other decoupling schemes tested in this work.

A comparison of the linewidths of the three best decoupling sequences, COMARO, TPPM, and SPARC-16, are given in Table 2 for all three decoupler power levels. As expected, the linewidths obtained by using SPARC-16 decoupling are smaller than those of the other two sequences at all values of $\gamma B_2/2\pi$. It is of interest to note that the linewidths for TPPM and SPARC-16 decoupling do not decrease further when the decoupling power is increased from 19 to 22 kHz, suggesting that the linewidths in the decoupled spectra have reached their limit. Furthermore, the linewidths of the quaternary carbons 1 and 3′ actually increase when the decoupler power for SPARC-16 decoupling is increased. This is due to the effect of RF heating (*21*), which causes the order parameter of the liquid crystal to fluctuate, affecting the quaternary carbons the most because they have the largest chemical shift anisotropy. This result underscores the importance of using low decoupling power for the study of liquid crystals.

We also want to mention that the decoupling efficiency shows a significant dependence on the decoupler frequency offset for SPARC-16 and all the other decoupling sequences tested. For example, the peaks of the β and γ carbons are barely resolved in only one of the spectra shown (Fig. 1j, III). They are better resolved when the decoupler offset is increased by about 300 Hz, but the peak of the ω carbon becomes broader in the mean time. Unfortunately, because of the presence of a large chemical shift range and extensive dipolar coupling for the protons, it is difficult to quantify the effect of the decoupler frequency offset on all the ^{13}C peaks in bulk liquid crystal samples.

Because of the remarkable improvement of the decoupling efficiency of SPARC-16, we have also tested its application to solids. However, it does not perform any better than the basic TPPM sequence. The reason is probably due to the short T_2 of solid samples, for which longer sequences are not effective. Similarly, we have found that a further extension of the SPARC sequences beyond 16 elements does not offer further improvement for decoupling liquid crystals. Perhaps for the same reason, we have also found that the WURST adiabatic frequency-sweeping decoupling method (*12–15*) does not work well for liquid crystals.

In summary, the new broadband decoupling sequence with small phase angle rapid cycling, SPARC-16, has been proven to be superior to other decoupling schemes for the liquid crystal 5CB. It is robust, easy to implement, and needs little calibration. The most important feature of this sequence is that it can achieve remarkable improvement at a sufficiently low decoupling power, suggesting that it will be very useful for liquid crystal systems, which are very susceptible to RF heating.

EXPERIMENTAL

All the experiments were carried out on a Varian Unity/ Inova 400 MHz NMR spectrometer equipped with a wave form generator for generating decoupling sequences. The experiments were performed at ambient temperature using a Varian magic angle spinning (MAS) probe without sample spinning. The reason for using the MAS probe was to obtain a reasonable B_2 field with small RF power ($\gamma B_2/2\pi = 13$ kHz for 16 W). To minimize RF heating, a very small duty cycle (1%) was used, with an overall cycling time of 4 s. The number of scans was 100 for each spectrum, and no line broadening was used for data processing.

REFERENCES

1. R. R. Ernst, *J. Chem. Phys.* **45,** 3845 (1966).

2. M. H. Levitt and R. Freeman, *J. Magn. Reson.* **43,** 502 (1981).

3. M. H. Levitt, R. Freeman, and T. Frenkiel, *J. Magn. Reson.* **47,** 328 (1982).

4. M. H. Levitt, R. Freeman, and T. Frenkiel, *J. Magn. Reson.* **50,** 157 (1982).

5. M. H. Levitt, R. Freeman, and T. Frenkiel, *in* ''Advances in Magnetic Resonance'' (J. S. Waugh, Ed.), Vol. 11, p. 47, Academic Press, New York (1983).

6. A. J. Shaka, J. Keeler, T. Frenkiel, and R. Freeman, *J. Magn. Reson.* **52,** 335 (1983).

7. A. J. Shaka, J. Keeler, and R. Freeman, *J. Magn. Reson.* **53,** 313 (1983).

8. A. J. Shaka, P. B. Barker, and R. Freeman, *J. Magn. Reson.* **64,** 547 (1985).

9. A. J. Shaka and J. Keeler, *Prog. NMR Spectrosc.* **19,** 47 (1987).

10. Z. Starcuk, Jr., K. Bartusek, and Z. Starcuk, *J. Magn. Reson. A* **107,** 24 (1994).

11. T. E. Skinner and M. R. Bendall, *J. Magn. Reson. A* **112,** 126 (1995).

12. Ē. Kupče and R. Freeman, *J. Magn. Reson. A* **115,** 273 (1995).

13. Ē. Kupče and R. Freeman, *J. Magn. Reson. A* **117,** 246 (1995).

14. Ē. Kupče and R. Freeman, *Chem. Phys. Lett.* **250,** 523 (1996).

15. Ē. Kupče and R. Freeman, *J. Magn. Reson. A* **118,** 299 (1996).

16. R. Fu and G. Bodenhausen, *Chem. Phys. Lett.* **245,** 415 (1995).

17. R. Fu and G. Bodenhausen, *J. Magn. Reson. A* **117,** 324 (1995).

18. R. Fu and G. Bodenhausen, *J. Magn. Reson. A* **119,** 129 (1996).

19. M. Mehring, ''High Resolution NMR Spectroscopy in Solids,'' Springer-Verlag, New York (1983).

20. A. E. Bennett, C. M. Rienstra, M. Auger, K. V. Lakshmi, and R. G. Griffin, *J. Chem. Phys.* **103,** 6951 (1995).

21. B. M. Fung, *J. Magn. Reson.* **86,** 160 (1990).

22. B. M. Fung, D. S. L. Mui, I. R. Bonnell, and E. L. Enwall, *J. Magn. Reson.* **58,** 254 (1984).

23. D. Suter, K. V. Schenker, and A. Pines, *J. Magn. Reson.* **73,** 90 (1987).

24. K. V. Schenker, D. Suter, and A. Pines, *J. Magn. Reson.* **73,** 99 (1987).

25. D. Suter, A. Pines, J. H. Lee, and G. Drobny, *Chem. Phys. Lett.* **144,** 324 (1988).

26. J. S. Waugh, *J. Magn. Reson.* **49,** 517 (1982).